

Quantum-Chemical Study on the Bioactive Conformation of Epothilones

Verónica A. Jiménez*

Departamento de Química Orgánica y Grupo de Química Teórica y Computacional, Facultad de Ciencias Químicas, Universidad de Concepción Casilla 160-C, Concepción, Chile

Received September 1, 2010

Herein, I report a DFT study on the bioactive conformation of epothilone A based on the analysis of 92 stable conformations of free and bound epothilone to a reduced model of tubulin receptor. The equilibrium structures and relative energies were studied using B3LYP and X3LYP functionals and the 6-31G(d) standard basis set, which was considered appropriate for the size of the systems under study. Calculated relative energies of free and bound epothilones led me to propose a new model for the bioactive conformation of epothilone A, which accounts for several structure–activity data.

1. INTRODUCTION

Epothilones A and B are 16-membered macrolide natural products (Figure 1), which have been widely studied as antitumor agents due to their ability to inhibit cell division by tightly binding to tubulin protein, blocking the disassembly of microtubules.^{1–5} Their high biological activity and improved water solubility have made epothilones attractive alternatives to paclitaxel in cancer treatment.⁶ In addition, their less complex molecular structure has promoted intensive research to develop practical synthetic routes for the production of epothilone analogues for biological evaluation. Since 1996, a huge number of epothilone analogues have been synthesized, but only a few of them have been recognized as potent and effective antitumor agents, despite their high chemical resemblance to the structure of active species.^{7–17}

Extensive research has focused on finding a suitable model for epothilone–tubulin binding; however, neither molecular modeling nor structure–activity relationship data have succeeded in providing an unambiguous picture of the binding mode of the drug to tubulin. First proposals were taken from the crystal structure of epothilones A and B, which share a common conformation in the macrolide ring but differ in the thiazole side-chain conformation due to its high conformational freedom.² MM Monte Carlo analysis and NMR spectroscopy data for epothilone A in aqueous solution afforded two major conformations for epothilones that differ in the position of C3-hydroxyl with respect to the macrolide plane and in the dihedral angle of the C6–C10 region.^{18,19} One of these conformations was observed to be identical to the solid state conformation of epothilones.^{18,19} In the search for a common pharmacophore for paclitaxel and epothilones, Snyder et al. proposed a bioactive conformation for EpoB, which possess an endo-orientation of the epoxide ring within the macrocycle in contrast to previous proposals.²⁰ Another quite distinct bioactive conformation was proposed by Poulos et al. on the basis of the crystal structure of epothilones B and D in complex with cytochrome P450.²¹ Using NMR, molecular modeling, and crystallography of epothilone A–tubulin complex in Zn²⁺ ions stabilized layers, Nettles et

al. proposed a conformation of epothilone with the epoxide ring in endo-orientation.^{22,23} In an alternative approach, Carlomagno et al. used NMR spectroscopy to elucidate the structure of epothilone A bound to nonpolymerized tubulin. The overall derived conformation is similar to the crystal structure of free epothilone, showing slight differences in the region C2–C3.^{24–26}

All previously described conformations account for specific structure–activity data, but some questions still remain unclear. For instance, proposed models do not explain why epothilones of the B series, which have a methyl substituent at C12, are generally more active than those of the A series.^{2,14} It is also not obvious why the removal of the C8 methyl group leads to a prominent reduction in activity.¹⁶

In this context, it becomes relevant to address the search for the bioactive conformation of epothilones by means of ab initio quantum-chemical calculations. The use of “first principle” methods can provide valuable information about structural factors that are involved in the stability of epothilone–tubulin system. In addition, ab initio computations have considerable advantages with respect to semiempirical or purely classical molecular mechanic approaches, because the absence of parameter-dependent results provides an unambiguous way to analyze the effect of chemical substitution on epothilone’s biological activity.

Until now, only three literature reports describe the use of quantum-chemical calculations in the study of epothilones’ conformation. In 1999, Ballone et al. presented a density-functional study of paclitaxel, taxotere, baccatin III, discodermolide, and epothilone A based on the geometry optimization of a single structure of each molecule in gas phase.²⁷ In 2008, Rusinska-Roszak et al. reported a compu-

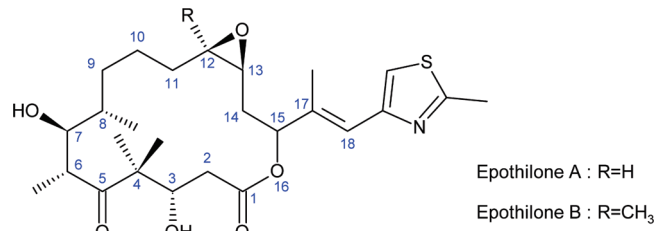


Figure 1. Structure of epothilones A and B.

* Corresponding author e-mail: veronicajimenez@udec.cl.

tational study of open-chain epothilone analogues in the gas phase based on B3LYP/6-31+G(d,p) calculations.²⁸ Their results showed a high conformational similarity between minimum energy conformers of open-chain analogues and the corresponding fragments of Taylor's reported structure for epothilone A in solution. Recently, in 2009, Rusinska-Roszak et al. applied the same level of theory to analyze the interconversion between endo- and exo-epoxide moieties in a simplified model of epothilone A.²⁹

All previously reported quantum-chemical studies have dealt with particular features of epothilone A and some analogues. However, none of them have dealt with the use of ab initio calculations neither in a systematic conformational search of epothilone's macrocycle nor in the study of the intermolecular interactions between tubulin receptor and epothilone to elucidate its preferred binding mode. Herein, I report a prototype quantum-chemical approach based on a series of density-functional computations on free and bound epothilones, considering a reduced model of the tubulin binding site. My results suggest that free epothilones can exist in several different conformations, but only few structures appear as suitable conformations for complexed epothilone, leading me to propose a new model for the bioactive conformation of epothilone A. To my knowledge, this is the first full ab initio computational study dealing with this subject.

2. COMPUTATIONAL ASPECTS

Structure Optimization of Epothilones. The 3D structure of epothilone A was constructed by modification of X-ray crystallography data.² The starting structure of epothilone A was fully optimized and subjected to a systematic conformational search at the PM3^{30,31} level of theory by scanning each dihedral angle within the macrocycle in 36 steps of 5°. For each fixed-dihedral, the other degrees of freedom are allowed to evolve to their minimum energy structure in an optimization procedure. From the 576 structures explored, I selected 50 minimum energy conformations with relative energies ranging from 0.0 to 10.0 kcal mol⁻¹. These 50 minimum energy structures were taken as starting geometries for a second conformational search at PM3 level by scanning each dihedral angle within the macrocycle in 36 steps of 5°. A total of 28 800 possible structures were analyzed at PM3 level, leading to 907 minimum energy conformations with relative energies between 0.0 and 10 kcal mol⁻¹. The set of 907 structures was subjected to full geometry optimization at the B3LYP/6-31G(d) level, leading to 73 different energy minima, with relative energies ranging from 0.0 to 10 kcal mol⁻¹ and 19 stable conformations with relative energies between 10 and 16 kcal mol⁻¹. During the optimization process, it was observed that many starting structures converged to a single closely related geometry, leading to a set of 92 minimum energy conformers of epothilone A. Vibration analysis at B3LYP/6-31G(d) level showed that these 92 conformers correspond to true energy minima. These structures were employed in further geometry optimization at X3LYP/6-31G(g)^{32–34} level and energy refinement procedures at B3LYP/6-311++G(d,p)//B3LYP/6-31G(d) and X3LYP/6-311++G(d,p)//X3LYP/6-31G(d) levels of theory.³⁵ SCRF calculations at B3LYP/6-31G(d) and X3LYP/6-31G(g) levels

were carried out to take into account solvent effects on the relative stability of epothilone conformers. The Polarizable Continuum Model (PCM) combined with the UAHF atom type option was employed to carry out my calculations in aqueous solution. Conformational search, geometry optimization, vibrational analysis, and SCRF calculations were performed with the Gaussian 03 package.³⁶

Tubulin polymerization properties reported by Nicolaou et al.³ were employed as activity data^{37,38} to analyze the suitability of each optimized conformation of epothilone A based on a geometric analysis of particular regions of the macrocycle.

Reduced Model of Tubulin Receptor. The crystalline structure of epothilone-bound tubulin in zinc-stabilized sheet solved at 2.9 Å resolution (1TVK)²³ was employed to construct a reduced model of the tubulin binding site. Molecular Dynamics (MD) calculations were carried out on the tubulin structure extracted from 1TVK to obtain an equilibrated conformation of the active site for further ab initio calculations. MD simulations were performed with NAMD software³⁹ and the all-atom CHARMM27⁴⁰ force field. TIP3 water model was employed to solvate the system under periodic boundary conditions in an isothermal–isobaric ensemble (NPT). Protonation states of all ionizable residues were set to those corresponding to pH 7.0, by using PROPKA 2.0.^{41,42} According to PROPKA results, three cationic residues (Lys19, Arg276, and Arg282) and two anionic residues (Glu22 and Asp224) are located in close proximity of complexed epothilone in 1TVK tubulin structure. A 10 ns simulation was carried out at a constant temperature of 300 K and pressure 1 bar using NAMD Nosé–Hoover implementations.

The resulting structure from MD calculations was employed to build a reduced model of tubulin receptor considering all amino acid residues located within 5.5 Å of epothilone, according to the complex model found in 1TVK. This reduced model contains 16 aminoacidic residues and a total charge of +1, according to the protonation states predicted by PROPKA. The C-terminal and N-terminal atoms were properly saturated with hydrogen atoms as reported in the literature. The obtained model was employed in further quantum-chemical calculations to identify the most stable conformation of epothilone bound to tubulin receptor.

Epothilone–Tubulin Complexes. Epothilone–tubulin complexes were built by placing each EpoA optimized conformer within the reduced model of tubulin receptor. The most appropriate epothilone starting location was considered to be the one that maximizes the overlapping between the 16-membered macrocycle of epothilone conformers and the corresponding atoms of EpoA complexed in the 1TVK model. Molecular alignment was performed by means of the Extended Orthogonal Procrustes (EOP) method,^{43–45} which provides the best matching between two structures, preserving their internal conformation. The best matching is defined as the one that minimizes the root-mean-square distance (rmsd) between epothilone conformers and the corresponding EpoA complexed in the 1TVK model.⁴⁶ The EOP method was implemented in a MATLAB 7.0⁴⁷ routine. The alignment algorithm was applied to obtain 92 starting structures for epothilone–tubulin complexes.

Epothilone–tubulin complexes were subjected to subsequent geometry optimization at the PM3, B3LYP/3-21G,

B3LYP/6-31G(d), and X3LYP/6-31G(d) levels of theory. X3LYP functional was selected to analyze the relative energy of epothilone–tubulin complexed due to its high performance in describing nonbonding intermolecular interactions.^{32,34} C and N atoms involved in peptidic bonds were fixed to retain the general structure of the active site. This choice is supported by the fact that the active site remains essentially unaltered after complexation, as argued by Carlomagno et al. in previous reports.²⁶ On the other hand, EpoA and all lateral chains were allowed to move along the optimization procedure. Calculated relative energies for epothilone–tubulin complexes were BSSE-corrected,^{48,49} using the counterpoise method as implemented in the Gaussian 03 package suite.

3. RESULTS AND DISCUSSION

Minimum Energy Conformers of Epothilone A.

a. Energetic Aspects. PM3 conformational search and geometry optimization at the B3LYP/6-31G(d) and X3LYP/6-31G(d) levels led me to identify 92 minimum energy conformers for epothilone A, with relative energies ranging from 0.0 to 16.0 kcal mol⁻¹, as reported in Table 1. Both B3LYP and X3LYP methods afford similar trends in calculated relative energies. Because of the presence polarizable atoms in epothilone, single point calculations at the B3LYP/6-311++G(d,p) and X3LYP/6-311++G(d,p) levels were employed to refine energy calculations (Table 1). Results obtained with a triple- ζ basis set with polarization and diffuse functions show only small changes in the observed relative energy trends as compared to 6-31G(d) basis set calculations. From these results, it was considered appropriate to employ the 6-31G(d) basis set in the remaining theoretical calculations.

According to my results, there are ~30 structures with relative energies <5 kcal mol⁻¹, which can be considered as equally probable conformational states for isolated epothilone A, given the margins of error of the theoretical methods herein employed. This result accounts for the intrinsic conformational flexibility of epothilones.^{3,18,24} Because gas-phase calculations are not representative of aqueous biological media, PCM calculations were performed at the B3LYP/6-31G(d) and X3LYP/6-31G(d) levels to study the relative stability of epothilone conformers in aqueous solution (Table 1). My results show that gas-phase relative energy trends are no longer retained in aqueous media. However, most of the stable conformations found in the gas phase have relative energies lower than 5 kcal mol⁻¹ in water. Again, compound **1** appears to be the most stable species within the group.

b. Structural Aspects. One distinctive feature of epothilone A minimum energy conformers is the orientation of the epoxide ring within the macrocycle, which determines their classification as endo-type or exo-type macrocycles (Figure 2). The structural examination of optimized conformations reveals that 69 conformations belong to the exo-type group, whereas only 23 can be classified as endo-type. According to the energetic data provided in Table 1, the most stable epothilone's conformers belong to the exo group.

To characterize the structure of optimized epothilone conformers, four dihedral angles corresponding to different regions of the macrocycle were analyzed and compared to the corresponding dihedrals extracted from previously reported bioactive conformations (Table 2). Direct comparison

between optimized and reported dihedrals suggests that the macrocycle structures of compounds **1**, **12**, **21**, **25**, and **44** are consistent with the crystalline structure of epothilone A.² These structures are essentially identical in the macrocycle conformation but differ in the relative orientation of the thiazole side chain. On the other hand, compounds **29**, **43**, and **66** appear to be comparable with the bioactive conformation proposed by Poulos et al. from the crystal structure of epothilone B bound to cytochrome P450.²¹ In addition, the bioactive conformation proposed by Carlomagno et al. from tubulin-bound epothilone NMR studies^{24–26} is well reproduced by conformers **18** and **77**. The unified model for epothilone and paclitaxel binding mode derived by Snyder et al.²⁰ is nicely reproduced by conformer **15**, which contains the described intramolecular hydrogen bond involving the epoxide moiety and the C3–OH group of epothilone's macrocycle. Finally, the bioactive species proposed by Nettles et al. from their crystallographic analysis of epothilone A–tubulin complex in Zn²⁺ ions stabilized layers is well reproduced by conformers **26**, **51**, and **72**. The fact that previously reported bioactive conformations are found within minimum energy conformers supports the validity of my conformational search, because it has explored relevant regions of the conformational space of epothilones.

According to the dihedral values reported in Table 2, there are several preferred conformations for each region of the macrocycle structure:

C1–C4 Region. Three main conformations were found in the C1–C4 region of the epothilone's macrocycle (Figure 3). In most cases, C1–C4 dihedrals range between 160° and 180°, describing approximate anti conformations, which are expected to be most stable and have been previously reported in the bioactive structures proposed by Poulos,²¹ Taylor,¹⁸ and Snyder.²⁰ Other conformers possess C1–C4 dihedrals close to 90°, which are consistent with the corresponding value reported for the bioactive conformation by Nettles et al.²³ The third relevant conformation corresponds to C1–C4 dihedrals close 60°, which describe approximate gauche conformations in this region.

A distinctive structural feature in the C1–C4 region is the orientation of the hydroxyl group attached to C3 (C3–OH). In most conformers, C3–OH is stabilized by intramolecular hydrogen bonds with appropriate hydrogen acceptors within the macrocycle. Four different hydrogen-bond patterns were found and are depicted in Figure 4. In the first case, the C3–OH is bound to the C1–carbonyl group with hydrogen-bond lengths ranging from 2.0 to 2.2 Å. This interaction is in agreement with the proposed pharmacophore for epothilones A and B and other antitumor agents by Ojima et al.⁵⁰ In the second arrangement, the C3–OH group is bound to the C5 carbonyl group, with hydrogen-bond distances between 1.8 and 2.0 Å. In the third motif, the C3–OH group is bound to O16, with bond lengths close to 2.0 Å. In this last pattern, the C3–OH forms an intramolecular hydrogen bond with the epoxide ring as described by Snyder et al. in their proposed bioactive conformation for epothilones.²⁰

Experimental evidence indicates that inversion of configuration at C3 is detrimental for the biological activity of epothilones,^{3,25} which suggests that C3–OH participates in specific intermolecular interactions with tubulin receptor. However, the fact that (*E*)-3-deoxy-2,3-didehydroepothilones,

Table 1. Calculated Relative Energies (kcal mol⁻¹) for Gas-Phase, Aqueous Solution, and Tubulin-Bound Epothilone Conformers^a

conformer	type	calculated relative energies (kcal mol ⁻¹)							
		gas-phase epothilones				solution-phase epothilones		epothilone–tubulin complexes	
		B3LYP/ 6-31G(d)	B3LYP/ 6-311++G(d,p)	X3LYP/ 6-31G(d)	X3LYP/ 6-311++G(d,p)	B3LYP/ 6-31G(d)	X3LYP/ 6-31G(d)	B3LYP/ 6-31G(d)	X3LYP/ 6-31G(d)
1	exo	0.0	0.0	0.2	0.0	0.0	0.0	28.8	29.5
2	exo	0.1	1.3	0.0	1.1	7.1	6.8	19.7	21.4
3	exo	0.1	0.1	0.2	0.0	2.8	2.2	28.5	30.1
4	exo	0.6	0.9	0.6	0.8	4.6	4.8	0.0	0.0
5	exo	0.7	1.2	0.7	1.0	2.9	2.9	35.0	30.3
6	exo	0.8	1.4	0.8	1.3	4.4	4.1	22.1	22.3
7	exo	0.8	2.7	0.5	2.2	7.6	7.5	8.9	7.3
8	exo	0.8	2.1	0.9	2.0	3.7	3.5	44.6	44.7
9	exo	1.2	2.0	1.3	2.0	4.0	4.0	7.7	9.6
10	exo	1.2	2.1	1.3	2.0	4.0	4.0	4.7	6.7
11	exo	1.7	1.4	1.8	1.3	2.7	2.8	30.6	30.1
12	exo	1.9	1.0	2.2	1.0	1.5	1.7	38.7	38.9
13	exo	2.1	2.8	2.0	2.6	8.3	8.2	31.0	31.2
14	exo	2.1	1.4	2.2	1.3	7.2	7.3	36.5	32.0
15	endo	2.8	3.7	2.6	3.3	6.6	6.5	35.8	33.5
16	endo	2.9	3.1	2.8	2.7	6.1	6.1	40.1	36.8
17	exo	3.0	3.7	3.0	3.2	6.4	6.3	10.6	10.2
18	exo	3.0	2.4	3.1	2.3	2.7	2.8	1.4	1.1
19	exo	3.1	2.1	3.4	2.2	4.5	4.6	8.2	8.3
20	exo	3.1	2.2	3.4	2.2	4.6	4.6	10.9	10.8
21	exo	3.2	2.5	3.5	2.5	1.2	1.3	49.5	46.0
22	exo	3.4	3.7	3.6	3.7	2.1	2.5	23.7	24.2
23	exo	3.5	3.1	3.7	3.2	4.1	4.5	13.5	13.5
24	exo	3.5	2.1	3.7	2.1	5.9	5.9	28.3	29.7
25	exo	3.5	2.2	3.8	2.2	1.7	1.8	18.8	18.8
26	endo	3.6	5.3	3.4	4.9	7.9	8.1	2.0	1.6
27	endo	3.6	5.3	3.4	4.9	8.3	8.1	35.5	28.5
28	exo	3.9	3.8	3.9	3.6	5.1	5.0	2.8	3.0
29	exo	4.2	3.4	4.1	3.9	4.6	4.8	7.6	7.5
30	exo	4.2	3.2	4.5	3.3	3.3	3.4	0.2	0.5
31	exo	4.2	3.9	4.5	4.0	4.7	4.5	22.1	21.5
32	exo	4.5	4.4	4.6	4.3	4.8	4.6	26.8	26.2
33	exo	4.8	5.4	4.8	5.3	7.4	7.2	7.3	7.6
34	endo	4.8	5.0	4.6	4.6	6.9	7.0	35.6	38.9
35	endo	4.9	6.4	4.7	6.1	8.9	8.8	10.4	10.2
36	exo	5.2	4.9	5.4	4.9	4.8	4.6	49.3	46.2
37	exo	5.2	4.9	5.4	4.9	4.9	4.8	17.2	17.7
38	exo	5.2	5.2	5.4	5.1	4.8	4.8	9.2	9.0
39	exo	5.7	7.2	5.3	6.7	14.9	14.2	21.3	20.8
40	exo	5.7	6.5	5.9	6.4	8.4	8.6	23.9	23.8
41	exo	5.8	6.0	5.8	5.8	7.4	7.3	6.3	6.8
42	exo	5.9	6.6	5.9	6.5	5.8	5.7	28.2	27.7
43	exo	6.0	6.2	6.2	6.2	6.0	6.1	22.2	22.1
44	exo	6.1	5.8	6.4	5.8	4.4	4.6	42.8	42.3
45	endo	6.3	8.3	5.9	7.8	10.1	10.5	34.5	34.1
46	exo	6.6	6.3	6.8	6.2	7.5	7.8	44.2	36.2
47	exo	6.6	6.6	6.8	13.3	8.4	8.2	24.6	23.1
48	exo	6.7	6.3	6.9	6.3	5.7	5.6	37.8	38.0
49	exo	6.9	7.7	7.0	7.6	6.4	6.4	31.7	32.3
50	exo	7.0	6.0	7.2	6.0	5.0	5.2	28.8	29.3
51	endo	7.1	9.1	6.8	8.6	12.6	12.1	36.1	34.9
52	endo	7.2	8.7	7.0	8.4	7.7	7.5	29.2	28.4
53	exo	7.3	7.2	7.6	7.3	5.4	5.5	6.3	6.6
54	exo	7.4	6.9	7.6	7.3	5.1	5.2	8.1	8.2
55	exo	7.5	6.9	7.7	6.9	6.4	6.4	22.7	23.1
56	exo	7.6	8.4	7.6	8.2	9.9	9.7	35.1	34.1
57	exo	7.8	8.8	7.9	8.7	12.0	12.2	31.1	30.8
58	endo	7.9	8.1	7.8	7.8	8.5	8.7	35.5	38.1
59	endo	8.0	7.4	8.0	7.3	11.4	11.0	1.9	2.5
60	exo	8.0	8.9	8.1	8.8	12.0	12.1	34.0	36.0
61	exo	8.3	8.1	8.4	8.1	9.6	9.6	36.2	37.2
62	exo	8.3	8.5	8.2	8.3	8.2	8.5	4.2	4.9
63	endo	8.3	8.6	8.3	8.4	10.1	10.3	23.0	22.8
64	exo	8.4	9.1	8.3	8.6	9.7	9.6	34.1	34.3
65	endo	9.3	9.3	9.1	9.0	12.6	12.3	34.3	33.3
66	exo	9.5	8.5	9.3	9.2	11.0	11.6	50.4	49.8
67	exo	9.6	8.0	9.3	9.5	8.4	8.2	36.9	37.8
68	endo	9.7	11.6	9.4	11.1	10.2	10.3	23.7	23.6

Table 1. Continued

conformer	type	calculated relative energies (kcal mol ⁻¹)							
		gas-phase epothilones				solution-phase epothilones		epothilone–tubulin complexes	
		B3LYP/ 6-31G(d)	B3LYP/ 6-311++G(d,p)	X3LYP/ 6-31G(d)	X3LYP/ 6-311++G(d,p)	B3LYP/ 6-31G(d)	X3LYP/ 6-31G(d)	B3LYP/ 6-31G(d)	X3LYP/ 6-31G(d)
69	exo	9.8	9.4	9.9	9.3	9.5	9.5	50.0	50.3
70	exo	10.0	9.8	10.1	9.7	9.0	9.4	23.7	24.6
71	exo	10.0	10.6	10.2	10.1	10.2	10.5	24.0	22.3
72	endo	10.4	11.5	10.3	11.2	12.0	12.0	22.3	21.8
73	endo	10.7	11.4	10.6	11.2	12.1	12.2	23.8	23.6
74	endo	11.1	11.6	11.0	11.3	12.4	12.1	29.0	29.8
75	exo	11.6	10.2	11.5	11.2	9.9	10.0	36.6	37.5
76	endo	11.7	12.0	11.6	11.8	12.7	12.5	39.9	38.1
77	exo	11.9	10.3	12.1	10.3	10.6	10.4	3.1	3.8
78	exo	12.1	10.2	12.4	10.2	8.3	8.3	24.1	23.9
79	exo	12.1	13.2	11.7	12.7	18.0	16.0	31.7	30.2
80	exo	12.5	11.8	12.7	11.9	11.2	11.5	17.9	18.2
81	endo	12.8	11.9	12.7	11.6	11.9	11.5	3.7	3.8
82	exo	12.9	13.7	12.5	13.3	16.9	16.5	41.0	41.5
83	endo	13.0	13.2	12.8	12.8	14.2	14.0	59.1	59.3
84	exo	13.1	11.6	13.2	11.4	9.7	10.5	27.2	23.9
85	exo	13.2	11.9	13.4	5.1	13.3	13.1	32.2	32.2
86	exo	13.7	13.1	3.0	3.2	19.5	19.0	5.2	4.4
87	exo	13.7	12.1	13.9	12.0	12.1	11.8	20.7	21.4
88	endo	14.2	13.5	14.1	13.3	12.2	12.3	16.4	16.1
89	endo	14.2	15.4	13.8	15.0	15.9	15.0	32.7	31.6
90	endo	14.2	14.5	14.4	14.4	12.8	12.0	24.0	23.8
91	endo	15.5	14.8	15.5	14.6	13.0	13.1	23.9	22.9
92	endo	15.9	15.1	15.9	14.8	14.7	14.9	30.1	30.2

^a Gas-phase geometry optimizations were performed at the B3LYP/6-31G(d) and X3LYP/6-31G(d) levels, followed by single point calculations with the 6-311++G(d,p) basis set. Aqueous solution calculations were performed at the B3LYP/6-31G(d) level with the PCM solvation model on B3LYP-optimized structures. Relative energies of epothilone–tubulin complexes were obtained by geometry optimization at the B3LYP/6-31G(d) and X3LYP/6-31G(d) levels.

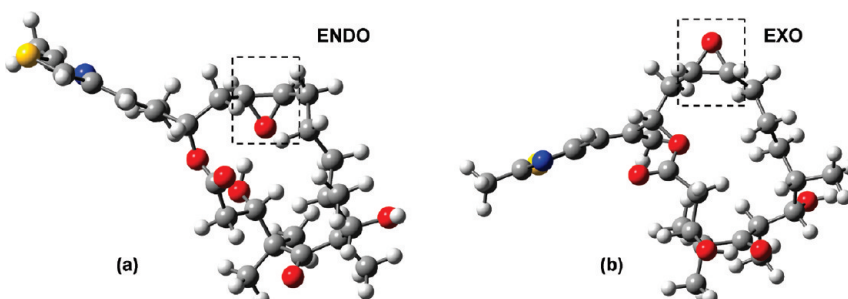


Figure 2. Representative structures of (a) endo-type and (b) exo-type conformers of epothilone A, based on the relative orientation of the epoxide ring within the macrocycle.

which lack the hydroxyl group at C3, are still moderately active species^{3,25} led me to speculate that C3–OH can also take part in the stabilization of the bioactive conformation by means of intramolecular hydrogen bonds.

C5–C8 Region. Main conformations found in the C5–C8 region for optimized conformers of epothilone A are depicted in Figure 5. In the first set of structures, the C5–C8 dihedral describes approximate anti conformations, in agreement with the bioactive conformation proposed by Poulos et al.²¹ In most of these structures, the hydroxyl group bound to C7 (C7–OH) forms an intramolecular hydrogen bond with the C5 carbonyl group. In conformers **26** and **51**, this hydrogen bond is accompanied by the intramolecular interaction between the C5–carbonyl and C3–OH group, as described earlier. These intramolecular interactions contribute to the intrinsic stability of anti conformations in the C5–C8 region but do not preclude the involvement of C7–OH in intermolecular interactions with tubulin receptor, because the

oxygen atom of C7–OH still appears to be available to act as proton acceptor with proper hydrogen donors within the binding site. A different situation was found in conformer **61** where the intramolecular hydrogen bond occurs between the C7–OH and O–16 atoms, leading to a highly distorted macrocycle in which the C7–OH group is oriented in such a way that its intermolecular interaction with tubulin receptor is forbidden (see Figure S1 in the Supporting Information).

The second group of structures contains C5–C8 dihedrals close to 60°, in agreement with the crystal structure of epothilones² and the reports of Taylor,¹⁸ Carlomagno,²⁴ and Snyder.²⁰ In these species, the C7–OH group points outside the macrocycle and is available for interaction with tubulin receptor. Other minority conformations found in the C5–C8 region correspond to dihedrals close to 37° and 123° as shown in Figure 5. Again, the C7–OH group of these

Table 2. Selected Dihedral Angles (deg) from the Macrocyclic Structure of Optimized and Experimentally Determined Epothilone A Conformers^a

structure	dihedrals (deg)				structure	dihedrals (deg)			
	$\angle C1-C4$	$\angle C5-C8$	$\angle C9-C12$	$\angle C13-O16$		$\angle C1-C4$	$\angle C5-C8$	$\angle C9-C12$	$\angle C13-O16$
Optimized Conformers									
1	177.6	-65.7	176.1	-88.4	52	-173.4	-126.7	52.2	50.7
2	-174.8	-170.4	-177.2	-59.8	53	-177.3	-105.2	165.0	-61.6
3	88.3	-61.3	156.7	-58.3	54	178.9	-123.4	169.6	-61.5
4	177.6	-166.5	175.7	-64.1	55	-176.5	-62.6	-86.7	-53.4
5	-64.4	-65.0	165.7	-171.4	56	163.4	81.4	-174.0	-67.9
6	179.7	-170.3	179.7	-51.8	57	-75.9	-166.8	-173.7	167.0
7	172.7	-166.2	172.0	-65.1	58	165.2	-144.1	55.1	57.6
8	-78.3	-174.6	-175.9	-168.9	59	154.5	-76.3	-175.1	73.0
9	-176.9	-170.5	179.8	-59.7	60	-75.9	-166.9	-173.2	166.3
10	-176.9	-170.4	179.7	-59.7	61	168.9	174.9	105.3	-62.5
11	87.9	-61.0	157.0	-57.3	62	68.6	-152.1	-177.0	-127.1
12	166.8	-61.7	172.9	-76.6	63	177.8	-75.2	60.0	76.2
13	82.1	-168.4	170.6	-60.4	64	85.5	-177.5	177.6	-62.8
14	179.0	-169.3	-177.2	-67.0	65	147.8	45.5	52.1	64.9
15	161.9	-65.1	74.2	46.0	66	173.3	-160.7	-161.3	-71.3
16	164.5	-65.8	66.4	54.5	67	178.5	-169.4	-175.8	-60.5
17	83.7	-163.3	175.1	-62.7	68	164.0	103.1	65.0	46.3
18	-166.1	-58.7	168.0	-71.4	69	168.6	-62.3	-171.7	71.4
19	177.9	-167.8	175.4	-74.8	70	-178.1	-52.8	-149.8	-63.6
20	177.8	-167.3	175.6	-75.1	71	62.9	-142.4	72.1	-111.8
21	167.1	-61.4	173.9	-76.7	72	88.5	-151.0	54.5	72.2
22	-173.2	68.9	-169.4	-65.7	73	137.8	-146.5	51.0	58.8
23	178.9	-173.4	165.4	-84.5	74	98.6	-169.9	60.9	70.9
24	159.9	-64.3	174.1	-132.1	75	177.6	-172.3	176.8	-67.1
25	166.7	-61.8	173.7	-76.4	76	-126.3	-138.8	55.9	69.0
26	89.8	-166.2	60.1	72.5	77	165.9	-82.5	171.9	-64.5
27	89.7	-166.3	60.0	72.4	78	149.7	-60.0	-175.5	-83.9
28	52.2	-61.9	170.4	-51.9	79	-173.4	-178.8	-144.8	83.3
29	175.2	-167.3	-177.5	-80.0	80	175.8	-62.2	171.9	-89.8
30	170.5	-62.9	179.2	-135.2	81	148.0	-62.9	58.5	56.1
31	171.8	-173.3	61.3	-54.0	82	84.6	-71.3	158.3	77.7
32	93.5	-71.3	172.0	-59.1	83	154.3	-42.3	67.9	74.0
33	-88.6	-51.4	166.4	-160.1	84	76.8	-53.0	176.7	-138.9
34	166.5	-54.9	-79.4	57.9	85	131.5	-59.1	172.5	-179.5
35	88.1	-66.2	64.3	73.7	86	154.5	-68.8	109.1	80.7
36	-159.0	-62.6	170.0	-154.7	87	172.7	-52.8	-164.3	-74.9
37	-159.0	-62.7	169.8	-155.1	88	104.5	-67.6	67.7	72.2
38	94.9	-56.6	179.9	-80.2	89	89.8	-78.1	54.1	75.2
39	-176.2	-171.2	-145.0	84.4	90	-170.5	-141.5	59.8	68.1
40	-79.2	-164.7	169.1	-71.7	91	-65.3	-60.4	64.1	43.4
41	-88.6	-51.0	165.3	-159.5	92	149.2	-44.0	68.2	72.5
42	87.4	-54.9	56.7	-57.1					
43	178.3	-173.1	-172.1	-70.7					
44	172.2	-65.2	168.2	-78.0					
45	162.0	43.8	52.7	50.8					
46	-108.1	-57.7	176.9	-148.8					
47	84.3	-139.5	66.4	-51.1					
48	-173.1	49.5	165.8	-74.8					
49	174.7	36.8	167.6	-78.0					
50	174.4	-58.8	-79.2	-69.7					
51	90.3	-172.9	71.6	69.0					
Crystal Structure of Epothilone B Bound to Cytochrome P450 ²¹									
	-179.9		-166.8		-159.4		-79.1		
X-ray Structure ^{2,24}									
	165.4		-64.0		174.8		-82.6		
Tubulin-Bound NMR-Derived Conformation ²⁴									
	-152.5		-70.0		-178.0		-62.6		
Unified Model for Epothilone and Paclitaxel Binding Mode ²⁰									
	165.1		-64.0		71.3		47.7		
Bound Conformation Determined by Electron Crystallography ²³									
	92.6		-152.2		68.0		65.3		

^a Optimized structures correspond to B3LYP/6-31G(d) calculations.

structures does not participate in any intramolecular hydrogen bond and therefore is available to interact with tubulin receptor.

Experimental evidence indicates that a change in the C7 stereochemistry causes a significant loss in activity for epothilones.³ This fact suggests that C7-OH is involved in intermolecular interactions with tubulin receptor. According to my results, most epothilone conformations (with the exception of conformer **61**) allow the intermolecular interaction between C7-OH and the tubulin binding site, even when C7-OH forms an intramolecular hydrogen bond with the C5-carbonyl group.

C9–C12 Region. Two major conformations are found in the C9–C12 region. In most cases, the C9–C12 dihedral adopts values close to 180°, describing approximate anti conformations, which are in agreement with the crystal structure of epothilone² and the bioactive conformations proposed by Poulos²¹ and Carlomagno.²⁴ On the other hand, some species possess C9–C12 dihedrals that describe approximate gauche conformations, which are in agreement with the bioactive conformations proposed by Snyder²⁰ and Nettles²³ (Figure 6).

Structural analysis revealed that the conformation of C9–C12 determines the orientation of the methyl group

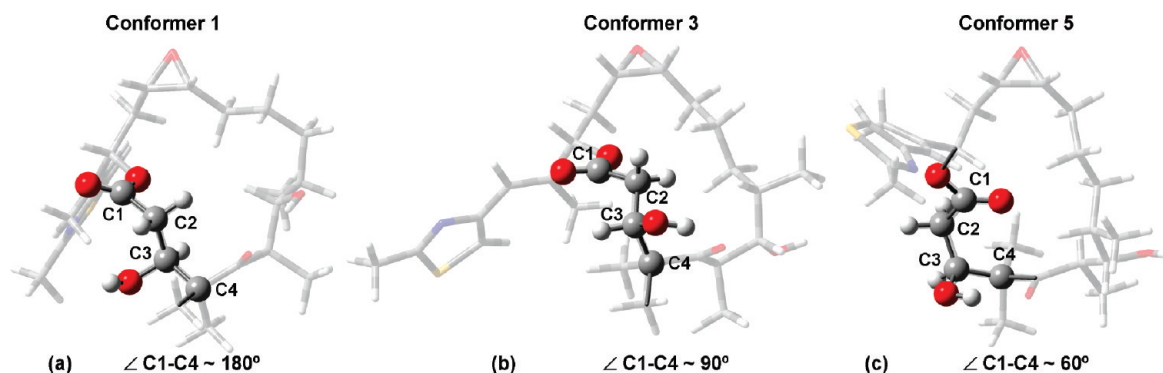


Figure 3. Representative structures of the conformations found in the region C1–C4 of epothilone's macrocycle. (a) The structure of conformer 1 shows a C1–C4 dihedral with an absolute value close to 180° , describing an approximate anti conformation. (b) In conformer 3, the C1–C4 dihedral is close to 90° . (c) In conformer 5, the C1–C4 dihedral takes an absolute value close to 60° , describing an approximate gauche conformation.

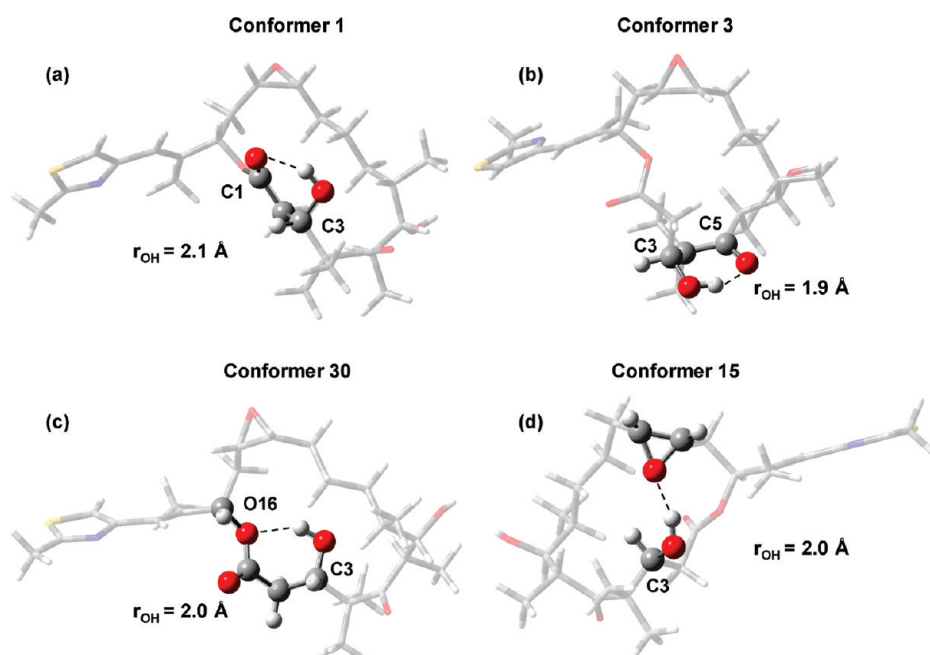


Figure 4. Intramolecular hydrogen bonds involving the C3–OH group. (a) Intramolecular hydrogen bond between C3–OH and C1 carbonyl. (b) Intramolecular hydrogen bond between C3–OH and C5 carbonyl. (c) Intramolecular hydrogen bond between C3–OH and O16. (d) Intramolecular hydrogen bond between C3–OH and epoxide oxygen atom.

attached to C8, which has been reported to be critical for the biological activity of epothilones.³ Experimental evidence has shown that the absence of the C8–methyl group or the inversion of configuration at C8 significantly reduces the biological activity of epothilones. This evidence suggests that the C8–methyl group is involved in hydrophobic interactions with tubulin receptor, which might be favored by the release of water molecules near the protein and ligand before binding. In this sense, a higher exposure of the C8–methyl group to the surroundings might favor the intermolecular interaction with tubulin receptor. My results show that the C8–methyl group points outside the macrocycle and appears to be available for intermolecular interaction in all conformers where the C9–C12 dihedral describes approximate anti conformations. On the other hand, conformations with C9–C12 dihedrals close to 60° orient their C8–methyl groups in such a way that they are less available for intermolecular interactions. According to the previous analysis, one can expect that conformers with C9–C12 dihedrals close to 60° are less appropriate to be considered as bioactive conformations of epothilone A.

Epoxide Region. The epoxide region shows major similarities among optimized conformers. Dihedral angles in this region are close to 0° for both endo and exo conformations. The most important structural difference in this region arises from the relative orientation of the epoxide ring respect to the macrocycle. In exo-type conformers, the epoxide ring points outside the macrocycle, whereas in endo conformations, the epoxide ring points inside the molecular ring. The four most stable epothilone's conformations are classified as exo conformers. In the most stable endo conformation (conformer 15), the epoxide oxygen atom participates in an intramolecular hydrogen bond with the C3–OH group, as described by Snyder et al.²⁰ in their proposed pharmacophore for epothilones and other related compounds (Figure 4d). The corresponding hydrogen-bond distance is 2.0 \AA , which is in the range of strong hydrogen-bonding interactions.

According to experimental evidence, the presence of the epoxide ring is not crucial for the biological activity of epothilones. Replacement of the epoxide ring by a Z-double bond leads to almost equally active species.⁵¹ Therefore, it seems reasonable to propose that epoxide oxygen atom is

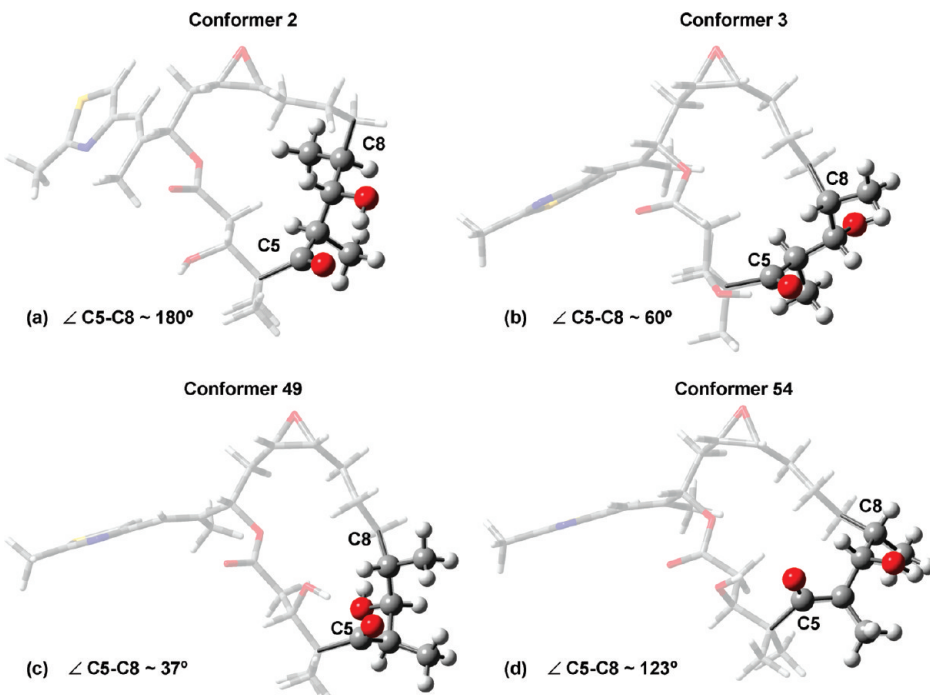


Figure 5. Representative structures of the conformations found in the region C5–C8 of epothilone's macrocycle. (a) In conformer 1, the C5–C8 dihedral is close to 180° . (b) In conformer 3, the C5–C8 dihedral adopts an absolute value close to 60° , describing an approximate gauche conformation. (c) In conformer 49, the C5–C8 dihedral takes a value close to 37° . (d) In conformer 54, the absolute value of C5–C8 dihedral is close to 123° .

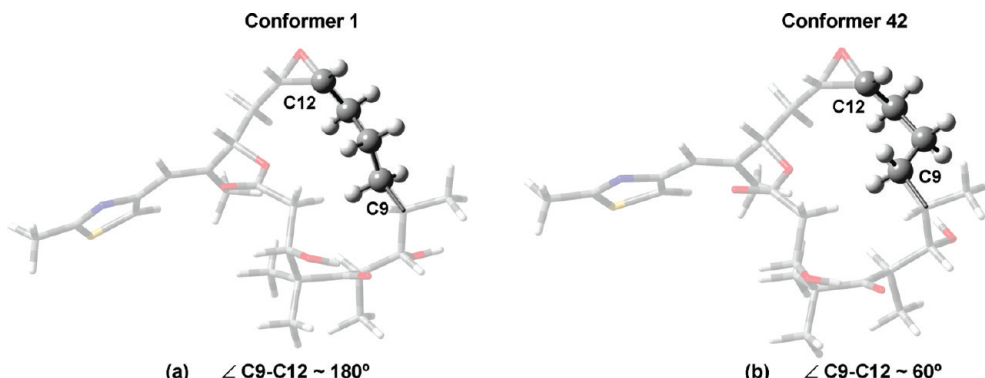


Figure 6. Representative structures of the conformations found in the region C9–C12 of epothilone's macrocycle. (a) In conformer 1, the C9–C12 dihedral adopts an absolute value close to 180° , describing an approximate anti conformation. (b) In conformer 42, the C9–C12 dihedral is close to 60° , describing an approximate gauche conformation.

not directly involved in intermolecular interactions with tubulin receptor.

C13–O16 Region. In most of the optimized conformers, the C13–O16 dihedrals describe approximate gauche conformations. Other minority conformations were found with C13–O16 dihedrals between 130° and 180° , describing approximate anti conformations.

According to my results, the conformation of C13–O16 determines the orientation of the epothilone's side chain that contains an olefinic spacer attached to a thiazole moiety. In some gauche structures, the methyl group attached to C17 is located above the macrocycle plane and appears to be in van der Waals contact with C4–methyl or C8–methyl groups as shown in Figure 7. In the remaining structures, the C17–methyl group points outside macrocycle and does not participate in any intramolecular interaction with other groups.

Experimental evidence indicates that substitution of C17–methyl by an ethyl group is associated with a signifi-

cant loss in biological activity.³ This fact leads me to propose that the C17–methyl group does not participate in direct intermolecular interaction with tubulin receptor, but is involved in intramolecular interactions within the epothilone macrocycle. In that case, the incorporation of an ethyl group at C17 could interfere in the intramolecular van der Waals interactions, leading to a less active species.

According to the previous analysis, there are some specific structural features within epothilone macrocycle that might favor its interaction with tubulin receptor. To test these hypotheses, the following section describes the results of a computational study on the intermolecular interaction between epothilone and tubulin receptor, based on a reduced model of the binding site.

Computational Study of Epothilone–Tubulin Interaction. A reduced model of the binding site was employed to study the epothilone–tubulin interaction considering the structure of 92 minimum energy conformers of epothilone A. Optimized geometries were obtained at the X3LYP/6-

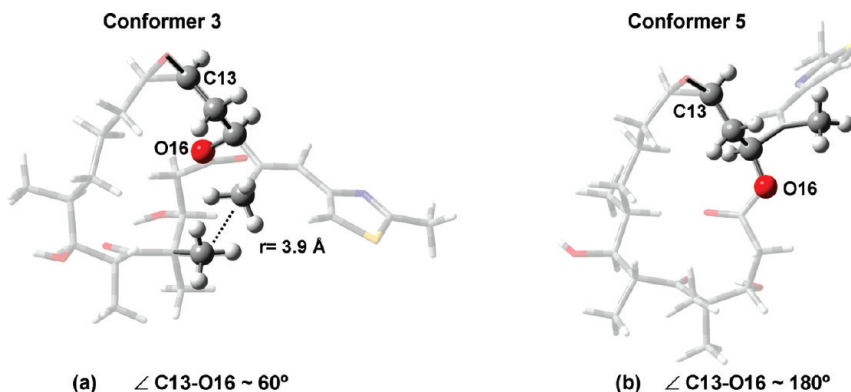


Figure 7. Representative structures of the conformations found in the region C13–O16 of epothilone's macrocycle. (a) In conformer 3, the C13–O16 dihedral adopts a value close to 60°, describing an approximate gauche conformation. (b) In conformer 5, the C13–O16 dihedral is close to 180°, describing an approximate anti conformation. Structure (a) shows the intramolecular interaction between C17–methyl and C4–methyl groups.

31G(d) level, due to the high performance of this method in describing nonbonding intermolecular interactions.^{32,34}

The structural analysis of optimized supramolecular complexes reveals that the active site remains essentially unaltered after complexation, and only small displacements in the lateral chains of amino acid residues are observed (see Figure S2 in the Supporting Information). This result supports the validity of employing a reduced model of the binding site in the study of the epothilone–tubulin interaction, at least as a first approach to deal with this subject. Similarly, the structure of bound epothilones does not differ significantly from the isolated starting conformer employed to build epothilone–tubulin complexes. Additionally, all bound ligands share the same region of the binding pocket as epothilone A in 1TVK structure.²³ This result is supported by the calculated heavy-atom rmsd between each optimized epothilone–tubulin complex and the starting geometry of the complex taken from 1TVK (see the Supporting Information). Even though the crystalline structure of the epothilone–tubulin complex²³ may not be optimal due to its low resolution, the location of the ligand is well-defined. Therefore, the fact that my computational study predicts epothilone to occupy the same region of the tubulin receptor validates the employed methodology.

As a first approach to the energetic aspects of epothilone–tubulin binding, relative energies of 92 optimized epothilone–tubulin complexes (kcal mol⁻¹) were calculated at the B3LYP/6-31G(d) and X3LYP/6-31G(d) levels of theory (Table 1). X3LYP results were employed to analyze energy trends within epothilone–tubulin complexes due to its high performance in describing intermolecular interactions. According to these results, there are 10 complexes (**4**, **18**, **26**, **28**, **30**, **59**, **62**, **77**, **81**, **86**) with relative energies lower than 5.0 kcal mol⁻¹ that can be considered as equally stable, given the margin of error of energy calculations at the X3LYP/6-31G(d) level of theory. The direct geometry optimization of the epothilone–tubulin complex taken from the 1TVK structure led to a system with relative energy of 31 kcal mol⁻¹. If one compares these results with calculated relative energies for isolated ligands (Table 1), it can be observed that complexes **4**, **18**, **26**, **28**, and **30** contain conformers with relative energies below 5.0 kcal mol⁻¹. According to both energy criteria, conformers **4**, **18**, **26**, **28**, and **30** appear as the most probable binding models, under the theoretical

framework herein employed. However, the remaining minimum energy complexes cannot be discarded at this point.

Comparison between 10 minimum energy complexes and previously reported epothilone–tubulin models led me to the following results. Complexes **18** and **77** resemble the NMR-derived bioactive conformation of epothilone proposed by Carlomagno et al.,²⁴ whereas complex **26** is highly consistent with the bioactive conformation proposed by Nettles et al.²³ In the case of complex **30**, the conformation of epothilone's macrocycle is coherent with the NMR-derived bioactive conformation,²⁴ except in the C13–O16 region. On the other hand, the macrocycle conformation of epothilone in complexes **59** and **81** is quite similar to the proposed bioactive conformation by Snyder et al.²⁰ In the last case, the epoxide moiety is not involved in any intramolecular hydrogen-bonding interaction. Finally, the epothilone structures found in complexes **4**, **28**, **62**, and **86** do not have noticeable resemblance with previously reported bioactive conformations. Structural details about the 10 most stable epothilone–tubulin complexes are provided next.

Figure 8 contains the structure of complex **4**, which is the most stable epothilone–tubulin complex within the set of optimized structures. In the bound conformation of epothilone, the thiazole side chain has undergone a conformational reorganization that interrupts the intramolecular hydrogen bond between C3–OH and C1–carbonyl and reorients the C3–OH group to interact with the N atom of the thiazole ring as hydrogen acceptor (Figure 8). This intramolecular interaction accounts for the importance of C3–OH stereochemistry and a nitrogen heterocycle connected to the macrocycle by an olefinic spacer, which have been described to be critical for the biological activity of epothilones.^{3,25,52} This result is also in agreement with my previous hypothesis about the role of C3–OH in the stabilization of the bioactive conformation by means of intramolecular hydrogen bonds. The hydrogen bond between C3–OH and the thiazole N atom was not observed in any isolated epothilone conformer, and thus is expected to be proper of tubulin bound epothilones. The thiazole side-chain reorganization has a second structural consequence, which is the establishment of an intramolecular van der Waals contact between C17–methyl and C8–methyl groups (Figure 8). This interaction is coherent with experimental evidence that shows the importance of C8–methyl and its stereochemistry in the biological activity of epothilone

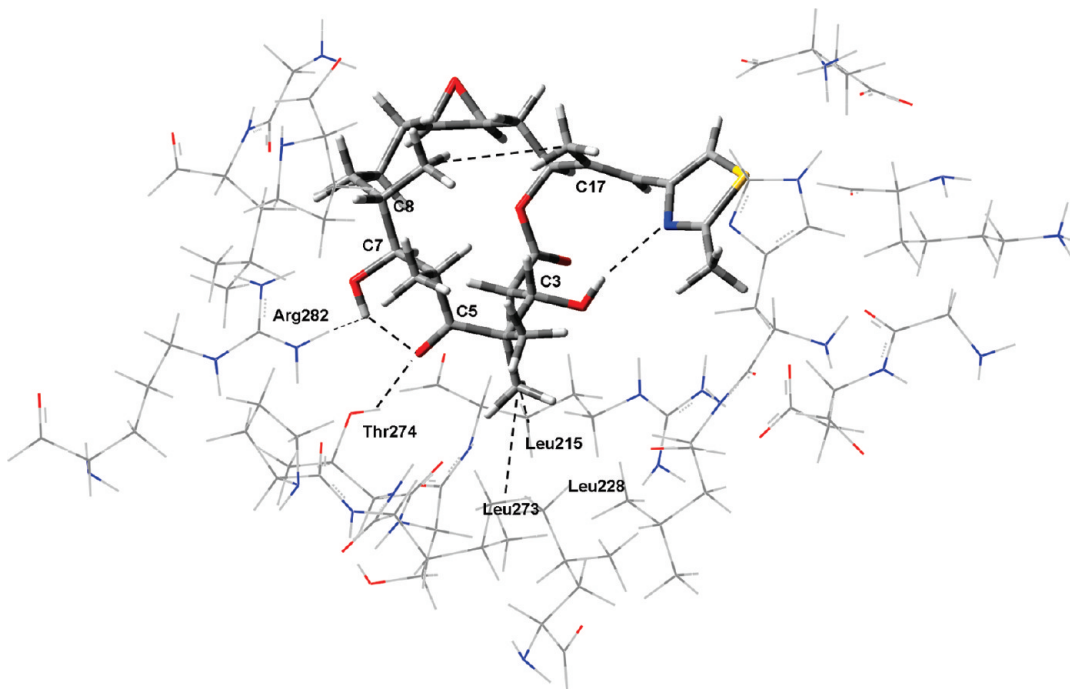


Figure 8. Structure of complex **4**. Some relevant intramolecular and intermolecular interactions are highlighted. The optimized geometry was obtained at the X3LYP/6-31G(d) level of theory.

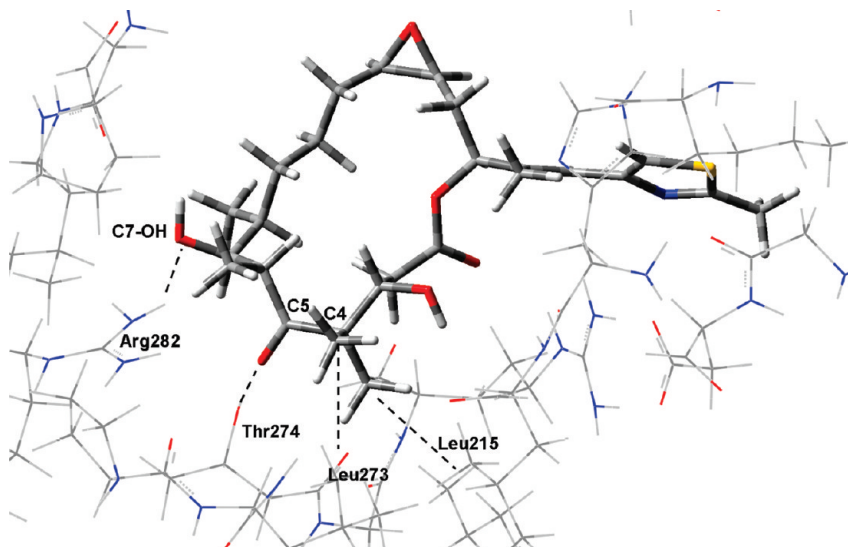


Figure 9. Structure of complex **18**. The optimized geometry was obtained at the X3LYP/6-31G(d) level of theory. Some relevant intermolecular interactions are highlighted.

derivatives.³ Additionally, the fact that substitution of C17-methyl by an ethyl group causes a significant loss in biological activity³ supports the existence of a stabilizing van der Waals contact between C17-methyl and C8-methyl in the bound conformation of epothilone, because this interaction might be interrupted if C17-methyl is replaced by an ethyl group. Besides intramolecular features, complex **4** shows the anchorage of epothilone to tubulin through the interaction of C4-methyl, C5-carbonyl, and C7-OH groups with appropriate residues of the binding pocket (Figure 8). C4-methyl interacts with leucine residues by means of van der Waals forces. On the other hand, C5-carbonyl and C7-OH groups act as hydrogen acceptors in intermolecular hydrogen bonds with Thr274 and Arg282, respectively. These interactions do not interrupt the intramolecular hydrogen bond between C7-OH and C5-carbonyl

found in the structure of isolated epothilone. The epoxide region of bound epothilone is located outside the binding pocket and does not seem to participate in any intermolecular interaction with tubulin receptor. This result is in agreement with the fact that chemical modifications in the C9-C15 region of epothilone are well tolerated.⁵¹ Finally, there is no evidence of hydrogen bonds or $\pi-\pi$ interactions between the thiazole moiety and His227,²⁶ because both rings reside far away in the binding site. According to my analysis, the bound conformation of epothilone in complex **4** can be considered as suitable bioactive conformation for epothilone A, under the theoretical framework herein employed.

The structure of complex **18** (Figure 9) is in high agreement with the NMR-derived conformation of epothilones.²⁶ Besides the macrocycle conformation, my model reproduces two experimental observations regarding

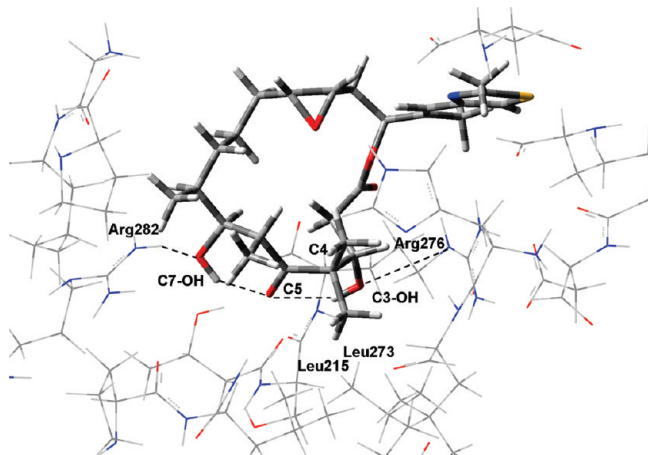


Figure 10. Structure of complex **26**. The optimized geometry was obtained at the X3LYP/6-31G(d) level of theory. Some relevant intramolecular and intermolecular interactions are depicted.

the epothilone–tubulin interaction. First, the C3–OH group of epothilone is not involved in intermolecular interactions with tubulin. Second, the positively charged residue Arg282 interacts with the C7–OH group of bound epothilone. In addition, complex **18** shows an intermolecular hydrogen bond between C5–carbonyl and Thr274, whereas the C4–methyl group interacts with leucine residues. From this structure, it is not clear why the substitution of C17–methyl by an ethyl group is detrimental for epothilone activity,³ because C17–methyl is not involved in any intra- or intermolecular interaction. Finally, the thiazole moiety is located in proximity of His227 but does not seem to be involved in intermolecular hydrogen bonds or π – π interactions with this residue, as proposed in the literature.²⁶ Both rings are 7 Å apart in complex **18**.

The structure of complex **26** is highly similar to the bioactive conformation proposed by Nettles et al. from crystallography data.²³ The intermolecular hydrogen bond between C7–OH and Arg282 is well reproduced by my model, as well as the hydrophobic contacts between C4–methyl and C8–methyl with proper apolar residues of the binding pocket. The main difference from the reported structure arises from the intermolecular interaction involving C3–OH and Thr274, which was not observed in my optimized complex. Instead of this interaction, my model shows an electrostatic contact between C3–OH and the positively charged Arg276 residue (Figure 10). The main drawback of this model is the lack of consistency with the fact that (*E*)-3-deoxy-2,3-didehydroepothilones are moderately active species^{3,25} In addition, it is not clear why the incorporation of an ethyl group at C17 causes a significant loss in biological activity.³ It is interesting to note that the bound conformation of epothilone retains the simultaneous intramolecular hydrogen bonds found in the isolated structure of conformer **26**, involving C5–carbonyl, C3–OH, and C7–OH groups (Figure 10).

In complex **28**, the C3–OH group is involved in both intra- and intermolecular interactions, with C5–carbonyl and Arg276, respectively (Figure 11). In addition, there is an intermolecular hydrogen bond between C7–OH and Arg282. The remaining epothilone–tubulin contacts are primarily hydrophobic due to C4–methyl and C6–methyl groups. Again, C17–methyl does not participate in intra- or inter-

molecular interactions. Similar features are found in complex **30**, except for C3–OH, which only participates in an intramolecular hydrogen bond with O16 (Figure 12).

Complexes **59** and **81** contain an endo-conformer of bound epothilone that resembles the bioactive conformation proposed by Snyder et al.²⁰ (Figure 13). Three main differences are found between these structures. First, complex **59** contains an intramolecular hydrogen bond between C3–OH and the epoxide moiety, as previously described.²⁰ Second, complex **81** shows an intermolecular interaction between C5–carbonyl and Thr274 that is not observed in complex **59**. Third, in complex **81**, there is evidence of π – π stacking interactions between the thiazole ring of epothilone and the His227 side chain as previously described in the literature.²⁶ In both complexes **59** and **81**, C7–OH is involved in an intermolecular hydrogen bond with the positively charged Arg282 residue. The remaining interactions are primarily hydrophobic due to C4–methyl and C6–methyl groups. Again, C17–methyl does not seem to be involved in any intra- or intermolecular interaction.

The structures of complexes **62** and **77** only show the intermolecular interaction between C7–OH and Arg282. In the case of complex **86**, the most distinctive intermolecular interaction is the apparent π – π stacking between the thiazole ring of epothilone and the His227 side chain.²⁶ None of these structures accounts for structure–activity data on the biological activity of epothilones (Figure 14).

The previous analysis suggests that the structure of the bound ligand in complex **4** can be considered as a new suitable model for the bioactive conformation of epothilone A. This structure accounts better for structure activity data than other proposed bioactive species. The validity of this new model needs to be tested by further theoretical work. In particular, I am focused on evaluating the effect of chemical modifications on the conformational properties of epothilone A and on the epothilone–tubulin intermolecular interaction. Unfinished work has shown an enhancement of the complex stability after incorporation of a methyl group at C12, which is coherent with the fact that epothilone B is a more active species as compared to epothilone A. Other structural modifications still in progress are the removal of C8–methyl and dehydration at C3. Additionally, QM/MM calculations are to be performed to analyze the role of each particular amino acid residue in the intermolecular interaction between epothilone and tubulin receptor.

Other important issue that needs to be tackled is the computation of reliable binding free energies that take into account the epothilone–tubulin intermolecular interaction as well as the role of explicit solvent molecules in the binding process. Solvent effects might be relevant because partial desolvation of the ligand is required to place epothilone inside the hydrophobic pocket of the tubulin receptor. Preliminary calculation of desolvation free energies with continuum solvation models (Table S2 in the Supporting Information) has shown that the desolvation process of most epothilone conformers is not spontaneous ($\Delta G > 0$) and must be driven by specific intermolecular interactions between epothilone and its binding site to overcome this free energy gain. On the other hand, some epothilone conformers are stabilized by desolvation ($\Delta G < 0$). For these species, the ligand desolvation constitutes a driving force for the binding process. The fact that different conformers experience

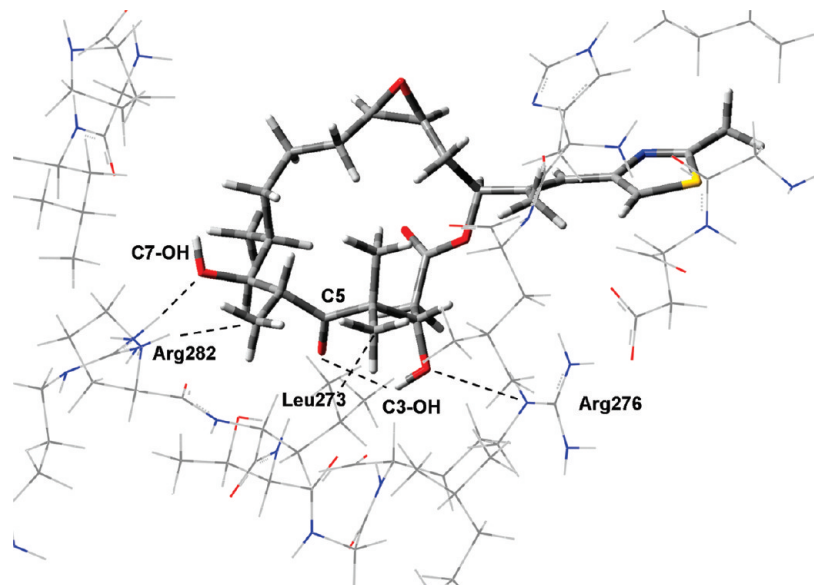


Figure 11. Structure of complex **28**. The optimized geometry was obtained at the X3LYP/6-31G(d) level of theory. Some relevant intermolecular interactions are highlighted.

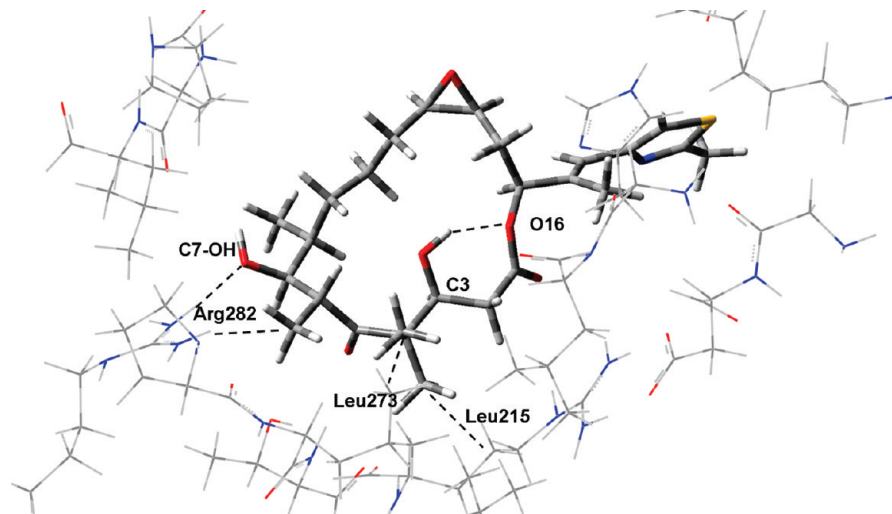


Figure 12. Structure of complex **30**. The optimized geometry was obtained at the X3LYP/6-31G(d) level of theory. Some relevant intramolecular and intermolecular interactions are highlighted.

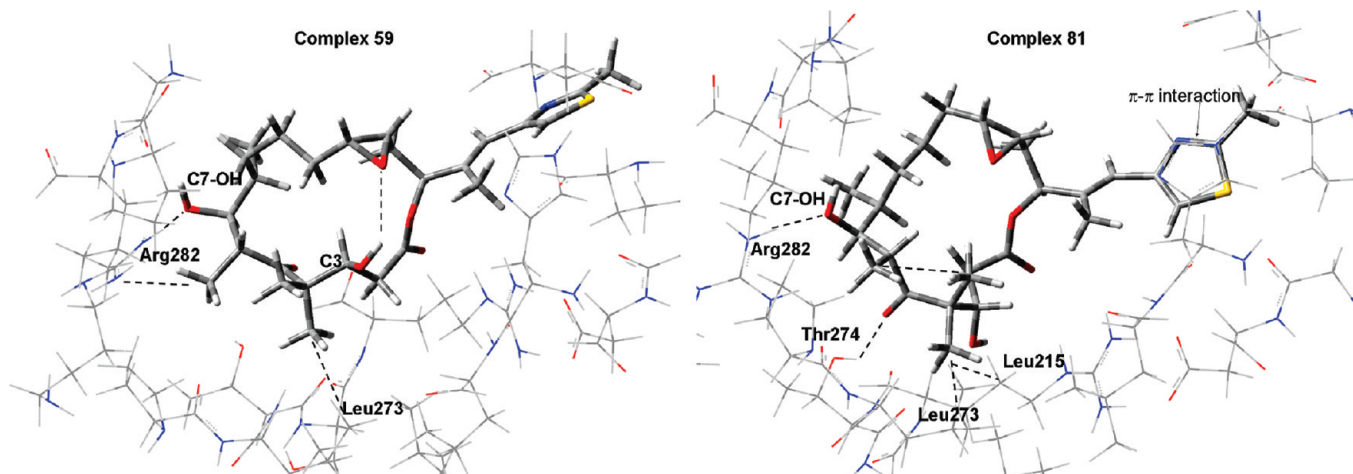


Figure 13. Structures of complexes **59** and **81**. The optimized geometries were obtained at the X3LYP/6-31G(d) level of theory. Some relevant intramolecular and intermolecular interactions are highlighted.

opposite free energy changes as a consequence of desolvation might play a crucial role in determining which structure

constitutes a better bioactive species. This issue will be addressed in a future report.

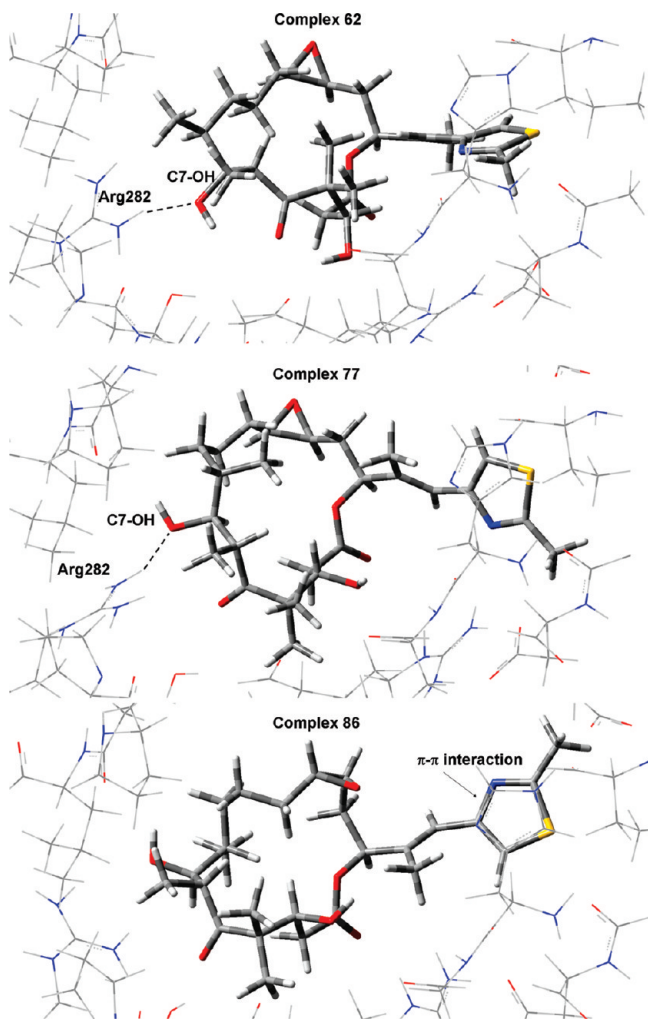


Figure 14. Structures of complexes **62**, **77**, and **86**. The optimized geometries were obtained at the X3LYP/6-31G(d) level of theory. Some relevant intramolecular and intermolecular interactions are highlighted.

CONCLUSION

The analysis of stable conformations of free and bound epothilone led me to identify 10 minimum energy epothilone–tubulin complexes with relative energies below 5 kcal mol⁻¹. Within this group, there are five structures (complexes **4**, **18**, **26**, **28**, and **30**) that contain epothilone conformers with relative energies <5 kcal mol⁻¹ in their isolated form. The structure of complex **26** is highly consistent with the interaction model proposed by Nettles et al.,²³ whereas complex **18** resembles the proposed bioactive conformation by Carlomagno et al.²⁴ The macrocycle conformation found in complex **30** is also in agreement with this structure except in the C13–O16 region. Thus, complexes containing conformers **4** and **28** constitute new models for epothilone–tubulin binding.

Structure–activity data led me to propose that complex **4** is the most suitable epothilone–tubulin complex within the species considered in the present study. According to my results, the intramolecular interaction between C3–OH and the N atom of the thiazole side chain stabilizes the presumed bioactive conformation and accounts for the importance of C3–OH stereochemistry and the nitrogen heterocycle connected to the macrocycle in the biological

activity of epothilones. On the other hand, the van der Waals contact between C17–methyl and C8–methyl groups accounts for the importance of C8 stereochemistry in the biological activity of epothilones. In addition, this interaction is helpful to understand why the incorporation of an ethyl group at C17 leads to a less active epothilone analogue. However, the analysis of structure–activity data is nonconclusive, and additional computational work needs to be done to prove the validity of the arguments herein stated. One important task is to obtain reliable binding energies considering the effect of explicit solvent molecules on the epothilone–tubulin interaction. In addition, it is necessary to analyze the effect of chemical modification of epothilone A on the conformational properties of isolated epothilones and on the binding interaction with tubulin receptor.

Future theoretical work could also be helpful to rationalize structure–activity data to provide a deeper understanding on the factors that control the epothilone–tubulin binding. A detailed description of the epothilone–tubulin interaction could lead to the development of improved and perhaps greatly simplified analogues for subsequent research. In this sense, the present work constitutes a starting theoretical approach to deal with the epothilone–tubulin complexation that can be taken as a model for how one might generally address problems of this type by means of quantum-chemical calculations.

In summary, within the context of the present study, complexes **4**, **18**, **26**, **28**, and **30** remain as viable binding candidates, given the double 5 kcal/mol relative energy cutoff. Complex **4** appears to be favored according to structure–activity data, and future work will provide tools to distinguish among them more thoroughly.

ACKNOWLEDGMENT

I thank FONDECYT Grant number 11070005 for financial support.

Supporting Information Available: Optimized geometries of epothilone conformers and epothilone–tubulin complexes. Stereoview of the most stable epothilone–tubulin complex. This material is available free of charge via the Internet at <http://pubs.acs.org>.

REFERENCES AND NOTES

- (1) Bollag, D. M.; McQueney, P. A.; Zhu, J.; Hensens, O.; Koupal, L.; Liesch, J.; Goetz, M.; Lazarides, E.; Woods, C. M. Epothilones, a new class of microtubule-stabilizing agents with a taxol-like mechanisms of action. *Cancer Res.* **1995**, *55*, 2325–2333.
- (2) Hofle, G. H.; Bedorf, N.; Steinmetz, H.; Schomburg, D.; Gerth, K.; Reichenbach, H. Epothilone A and B - Novel 16-membered macrolides with cytotoxic activity: Isolation, crystal structure, and conformation in solution. *Angew. Chem., Int. Ed. Engl.* **1996**, *35*, 1567–1569.
- (3) Nicolaou, K. C.; Roschangar, F.; Vourloumis, D. Chemical biology of epothilones. *Angew. Chem., Int. Ed.* **1998**, *37*, 2015–2045.
- (4) Mulzer, J.; Altmann, K. H.; Hofle, G.; Muller, R.; Prantz, K. Epothilones - A fascinating family of microtubule stabilizing antitumor agents. *C. R. Chim.* **2008**, *11*, 1336–1368.
- (5) Reichenbach, H.; Hofle, G. Discovery and development of the epothilones - A novel class of antineoplastic drugs. *Drugs Res. Dev.* **2008**, *9*, 1–10.
- (6) Goodin, S.; Kane, M. P.; Rubin, E. H. Epothilones: Mechanism of action and biologic activity. *J. Clin. Oncol.* **2004**, *22*, 2015–2025.
- (7) Balog, A.; Meng, D. F.; Kamenecka, T.; Bertinato, P.; Su, D. S.; Sorensen, E. J.; Danishefsky, S. Total synthesis of (-)-epothilone A. *Angew. Chem., Int. Ed. Engl.* **1996**, *35*, 2801–2803.

- (8) Nicolaou, K. C.; He, Y.; Vourloumis, D.; Vallberg, H.; Yang, Z. An approach to epothilones based on olefin metathesis. *Angew. Chem., Int. Ed. Engl.* **1996**, *35*, 2399–2401.
- (9) Su, D. S.; Meng, D. F.; Bertinato, P.; Balog, A.; Sorenson, E. J.; Danishefsky, S. J.; Zheng, Y. H.; Chou, T. C.; He, L. F.; Horwitz, S. B. Total synthesis of (−)-epothilone B: An extension of the Suzuki coupling method and insights into structure-activity relationships of the epothilones. *Angew. Chem., Int. Ed. Engl.* **1997**, *36*, 757–759.
- (10) Balog, A.; Harris, C.; Savin, K.; Zhang, X. G.; Chou, T. C.; Danishefsky, S. J. A novel aldol condensation with 2-methyl-4-pentenal and its application to an improved total synthesis of epothilone B. *Angew. Chem., Int. Ed.* **1998**, *37*, 2675–2678.
- (11) Sefkow, M.; Kiffe, M.; Hofle, G. Derivatization of the C12–C13 functional groups of epothilones A, B and C. *Bioorg. Med. Chem. Lett.* **1998**, *8*, 3031–3036.
- (12) Regueiro-Ren, A.; Borzilleri, R. M.; Zheng, X. P.; Kim, S. H.; Johnson, J. A.; Fairchild, C. R.; Lee, F. Y. F.; Long, B. H.; Vite, G. D. Synthesis and biological activity of novel epothilone aziridines. *Org. Lett.* **2001**, *3*, 2693–2696.
- (13) Regueiro-Ren, A.; Leavitt, K.; Kim, S. H.; Hofle, G.; Kiffe, M.; Gougoutas, J. Z.; DiMarco, J. D.; Lee, F. Y. F.; Fairchild, C. R.; Long, B. H.; Vite, G. D. SAR and pH stability of cyano-substituted epothilones. *Org. Lett.* **2002**, *4*, 3815–3818.
- (14) Nicolaou, K. C.; Sasmal, P. K.; Rassias, G.; Reddy, M. V.; Altmann, K. H.; Wartmann, M.; O’Brate, A.; Giannakakou, P. Design, synthesis, and biological properties of highly potent epothilone B analogues. *Angew. Chem., Int. Ed.* **2003**, *42*, 3515–3520.
- (15) Frein, J. D.; Taylor, R. E.; Sackett, D. L. New sources of chemical diversity inspired by biosynthesis: Rational design of a potent epothilone analogue. *Org. Lett.* **2009**, *11*, 3186–3189.
- (16) Balog, A.; Bertinato, P.; Su, D.-S.; Meng, D.; Sorenson, E.; Danishefsky, S. J.; Zheng, Y.-H.; Chou, T.-C.; He, L.; Horwitz, S. B. Stereoselective syntheses and evaluation of compounds in the 8-desmethylepothilone A series: Some surprising observations regarding their chemical and biological properties. *Tetrahedron Lett.* **1997**, *38*, 4529–4532.
- (17) Nicolaou, K. C.; Pratt, B. A.; Arseniyadis, S.; Wartmann, M.; O’Brate, A.; Giannakakou, P. Molecular design and chemical synthesis of a highly potent epothilone. *ChemMedChem* **2006**, *1*, 41–44.
- (18) Taylor, R. E.; Zajicek, J. Conformational properties of epothilone. *J. Org. Chem.* **1999**, *64*, 7224–7228.
- (19) Taylor, R. E.; Chen, Y.; Beatty, A.; Myles, D. C.; Zhou, Y. Q. Conformation-activity relationships in polyketide natural products: A new perspective on the rational design of epothilone analogues. *J. Am. Chem. Soc.* **2003**, *125*, 26–27.
- (20) Wang, M. M.; Xia, X. Y.; Kim, Y.; Hwang, D.; Jansen, J. M.; Botta, M.; Liotta, D. C.; Snyder, J. P. A unified and quantitative receptor model for the microtubule binding of paclitaxel and epothilone. *Org. Lett.* **1999**, *1*, 43–46.
- (21) Nagano, S.; Li, H. Y.; Shimizu, H.; Nishida, C.; Ogura, H.; de Montellano, P. R. O.; Poulos, T. L. Crystal structures of epothilone D-bound, epothilone B-bound, and substrate-free forms of cytochrome P450epoK. *J. Biol. Chem.* **2003**, *278*, 44886–44893.
- (22) Nettles, J. H.; Downing, K. H. The Tubulin Binding Mode of Microtubule Stabilizing Agents Studied by Electron Crystallography. In *Tubulin-Binding Agents: Synthetic, Structural and Mechanistic Insights*; Carlomagno, T., Ed.; Springer-Verlag: Berlin Heidelberg, 2009; Vol. 286, pp 209–257.
- (23) Nettles, J. H.; Li, H. L.; Cornett, B.; Krahn, J. M.; Snyder, J. P.; Downing, K. H. The binding mode of epothilone A on alpha,beta-tubulin by electron crystallography. *Science* **2004**, *305*, 866–869.
- (24) Carlomagno, T.; Blommers, M. J. J.; Meiler, J.; Jahnke, W.; Schupp, T.; Petersen, F.; Schinzer, D.; Altmann, K. H.; Griesinger, C. The high-resolution solution structure of epothilone A bound to tubulin: An understanding of the structure-activity relationships for a powerful class of antitumor agents. *Angew. Chem., Int. Ed.* **2003**, *42*, 2511–2515.
- (25) Erdelyi, M.; Pfeiffer, B.; Hauenstein, K.; Fohrer, J.; Gertsch, J.; Altmann, K. H.; Carlomagno, T. Conformational preferences of natural and C3-modified epothilones in aqueous solution. *J. Med. Chem.* **2008**, *51*, 1469–1473.
- (26) Reese, M.; Sanchez-Pedregal, V. M.; Kubicek, K.; Meiler, J.; Blommers, M. J. J.; Griesinger, C.; Carlomagno, T. Structural basis of the activity of the microtubule-stabilizing agent epothilone A studied by NMR spectroscopy in solution. *Angew. Chem., Int. Ed.* **2007**, *46*, 1864–1868.
- (27) Ballone, P.; Marchi, M. A density functional study of a new family of anticancer drugs: Paclitaxel, taxotere, epothilone, and discodermolide. *J. Phys. Chem. A* **1999**, *103*, 3097–3102.
- (28) Kamel, K.; Rusinska-Roszak, D. A computational study of open-chain epothilone analogue. *Int. J. Quantum Chem.* **2008**, *108*, 967–973.
- (29) Rusinska-Roszak, D.; Lozynski, M. De(side chain) model of epothilone: bioconformer interconversions DFT study. *J. Mol. Model.* **2009**, *15*, 859–869.
- (30) Stewart, J. J. P. Optimization of parameters for semiempirical methods I. Method. *J. Comput. Chem.* **1989**, *10*, 209–220.
- (31) Stewart, J. J. P. Optimization of parameters for semiempirical methods I. Method. *J. Comput. Chem.* **1989**, *10*, 221–264.
- (32) Su, J. T.; Xu, X.; Goddard, W. A. Accurate energies and structures for large water clusters using the X3LYP hybrid density functional. *J. Phys. Chem. A* **2004**, *108*, 10518–10526.
- (33) Xu, X.; Goddard, W. A. The X3LYP extended density functional for accurate descriptions of nonbond interactions, spin states, and thermochemical properties. *Proc. Natl. Acad. Sci. U.S.A.* **2004**, *101*, 2673–2677.
- (34) Xu, X.; Zhang, Q. S.; Muller, R. P.; Goddard, W. A. An extended hybrid density functional (X3LYP) with improved descriptions of nonbond interactions and thermodynamic properties of molecular systems. *J. Chem. Phys.* **2005**, *122*, 1–14.
- (35) Preliminary calculations revealed that increasing the size of the basis set does not induce any quantitative change in the optimized geometry of epothilone A. Optimized geometries and RMSD heavy-atom differences for tested epothilone conformers can be requested from the author. The B3LYP/6-311++G(d,p) method was employed to refine the energy calculation on structures that were probed to be unaltered as compared to B3LYP/6-31G(d). The use of single point calculations at B3LYP/6-311++G(d,p) is significantly cheaper in computational cost than optimization procedures at this level of theory, especially for the case of large systems as epothilones.
- (36) Frisch, M. J.; Schlegel, H. B.; Scuseria, G. E.; Robb, M. A.; Montgomery, J. A., Jr.; Vreven, T.; Kudin, K. N.; Millam, J. M.; Iyengar, S. S.; Tomasi, J.; Barone, V.; Cossi, M.; Scalmani, G.; Rega, N.; Petersson, G. A.; Hada, M.; Ehara, M.; Toyota, K.; Fukuda, R.; Ishida, M.; Nakajima, T.; Honda, Y.; Kitao, O.; Nakai, H.; Li, X.; Knox, J. E.; Hratchian, H. P.; Cross, J. B.; Bakken, V.; Jaramillo, J.; Gomperts, R.; Stratmann, R. E.; Yazyev, O.; Cammi, R.; Pomelli, C.; Ochterski, J. W.; Ayala, P. Y.; Voth, G. A.; Salvador, P.; Dannenberg, J. J.; Zakrzewski, V. G.; Daniels, A. D.; Strain, M. C.; Farkas, O.; Rabuck, A. D.; Raghavachari, K.; Foresman, J. B.; Cui, Q.; Baboul, A. G.; Clifford, S.; Cioslowski, J.; Liu, G.; Liashenko, A.; Piskorz, P.; Komaromi, I.; Fox, D. J.; Keith, T.; Al-Laham, M. A.; Peng, C. Y.; Challacombe, M.; Gill, P. M. W.; Johnson, B.; Wong, M. W.; Gonzalez, C.; Pople, J. A. *Gaussian 03*; Gaussian, Inc.: Wallingford, CT, 2004.
- (37) Lee, K. W.; Briggs, J. M. Comparative molecular field analysis (CoMFA) study of epothilones-tubulin depolymerization inhibitors: Pharmacophore development using 3D QSAR methods. *J. Comput.-Aided Mol. Des.* **2001**, *15*, 41–55.
- (38) Yuan, W.; Luan, L. B.; Li, Y. N. CoMFA 3D-QSAR analysis of epothilones based on docking conformation and alignment. *Chin. J. Chem.* **2007**, *25*, 453–460.
- (39) Phillips, J. C.; Braun, R.; Wang, W.; Gumbart, J.; Tajkhorshid, E.; Villa, E.; Chipot, C.; Skeel, R. D.; Kale, L.; Schulten, K. Scalable molecular dynamics with NAMD. *J. Comput. Chem.* **2005**, *26*, 1781–1802.
- (40) Foloppe, N.; MacKerell, A. D. All-atom empirical force field for nucleic acids: I. Parameter optimization based on small molecule and condensed phase macromolecular target data. *J. Comput. Chem.* **2000**, *21*, 86–104.
- (41) Bas, D. C.; Rogers, D. M.; Jensen, J. H. Very fast prediction and rationalization of pK(a) values for protein-ligand complexes. *Proteins* **2008**, *73*, 765–783.
- (42) Kieseritzky, G.; Knapp, E. W. Improved pK(a) Prediction: Combining Empirical and Semimicroscopic Methods. *J. Comput. Chem.* **2008**, *29*, 2575–2581.
- (43) Schoenemann, P. H. A generalized solution of the orthogonal Procrustes problem. *Psychometrika* **1966**, *31*, 1–10.
- (44) Schoenemann, P. H.; Carroll, R. Fitting one matrix to another under choice of a central dilation and a rigid motion. *Psychometrika* **1970**, *35*, 245–255.
- (45) Kroonenberg, P. M.; Dunn, W. J.; Commandeur, J. J. F. Consensus molecular alignment based on generalized procrustes analysis. *J. Chem. Inf. Comput. Sci.* **2003**, *43*, 2025–2032.
- (46) During EOP alignment, it was verified that the transformation that aligns epothilone structures is a pure rotation, because reflection is a forbidden operation when aligning molecular systems where stereochemistry should be preserved after any applied transformation.
- (47) *MATLAB, version 7.0*; The Mathworld Inc.: U.S., 2005.
- (48) Boys, S. F.; Bernardi, F. The calculation of small molecular interactions by the differences of separate total energies. Some procedures with reduced errors. *Mol. Phys.* **1970**, *19*, 553–566.
- (49) van Duijneveldt, F. B.; van Duijneveldt-van de Rijdt, J. G C M.; van Lenthe, J. H. State of the art in counterpoise theory. *Chem. Rev.* **1994**, *94*, 1873–1885.

- (50) Ojima, I.; Chakravarty, S.; Inoue, T.; Lin, S. N.; He, L. F.; Horwitz, S. B.; Kuduk, S. D.; Danishefsky, S. J. A common pharmacophore for cytotoxic natural products that stabilize microtubules. *Proc. Natl. Acad. Sci. U.S.A.* **1999**, *96*, 4256–4261.
- (51) Chou, T. C.; Zhang, X. G.; Balog, A.; Su, D. S.; Meng, D. F.; Savin, K.; Bertino, J. R.; Danishefsky, S. J. Desoxyepothilone B: An efficacious microtubule-targeted antitumor agent with a promising in vivo profile relative to epothilone B. *Proc. Natl. Acad. Sci. U.S.A.* **1998**, *95*, 9642–9647.
- (52) Bold, G.; Wojeik, S.; Caravatti, G.; Lindauer, R.; Stierlin, C.; Gertsch, J.; Wartmann, M.; Altmann, K. H. Structure-activity relationships in side-chain-modified epothilone analogues - How important is the position of the nitrogen atom. *ChemMedChem* **2006**, *1*, 37–40.

CI1003416